The Korean Journal of Ceramics, **6**[3] 304-308 (2000)

Improvement of Long-term Stability in SnO_2 Based Gas Sensor for Monitoring Offensive Odor

Jong Hun Park and Kwang Ho Kim

Department of Inorganic Materials Engineering, Pusan National University, Pusan 609-735, Korea
(Received September, 23, 1998)

WO_3/SnO_2 ceramics has been suggested as an effective sensing material for monitoring offensive odor or pollutant gases. This work was focussed on improving long-term stability, which has been a principal problem generally taking place in SnO_2 semiconductor gas sensor. Miniaturized thick film gas sensors were fabricated by screen printing technique. Two types of sensor materials, W doped SnO_2 and WO_3 mixed SnO_2, were comparatively investigated on those long-term stability and sensitivites to several gases. Small amount of W doping(0.1 mol%) into SnO_2 largely improved the long-term stability. The W(0.1mol%) doped SnO_2 gas sensor had higher sensitivities to both acetone and alcohol compared with WO_3(5 wt%) mixed SnO_2 gas sensor. On the contrary, WO_3(5 wt%) mixed SnO_2 gas sensor showed more superior sensitivity to cigarette smoke due to larger W content.

Keywords: Odor sensor, WO_3/SnO_2 ceramics, Long-term stablity, W-doping

I. Introduction

Semiconductor gas sensors are widely used for application in gas sensing. They offer many advantages such as simple fabrication, low cost, high sensitivity to both reducing and oxidizing gases, etc.

Odor sensing is one of the new trends in the application fields of semiconductor gas sensor because of the protection of the environment, the atmosphere in the work place and health science. Among the raw material of gas sensor, SnO_2 is the typical sensing material for air pollutant gases like formaldehyde, TMA, butyl acid, ethanol, etc.[1-5] On the other hand, WO_3 shows especially high sensitivity to H_2S gas which was typical offensive odor.[6-7] Therefore, the ceramic mixture consisting of both SnO_2 and WO_3 (5 wt%) has been suggested as an effective sensing material for monitoring air pollutant gases.[8]

It was, however, found that the gas sensor using the ceramic mixture of SnO_2/WO_3 had a problem of long-term stability. In actual use, the resistance of sensor steadily increased with operation time and finally the sensor was impossible to operate. The increase of resistance of SnO_2 sensing film is considered to be attributed to its conduction mechanism of nonstoichiometry because the nonstoichiometric oxides generally react with ambient oxygen. For an improvement of the long-term stability of SnO_2 based sensing film, it is considered to replace nonstoichiometric conduction mechanism with other conduction mechanism, for example controlled valence mechanism.

In this paper, W doped SnO_2 powder, in which Sn sites in SnO_2 crystal lattice was substituted for W ions, were prepared by coprecipitation method. The long-term stability and sensitivities to pollutant gases were comparatively investigated between W doped SnO_2 gas sensor and WO_3 mixed SnO_2 gas sensor.

II. Experimental Procedure

2.1. Preparation of sensing materials

To prepare the W doped SnO_2 powders for the gas sensor, the coprecipitation method was used. Fig. 1 shows manufac-

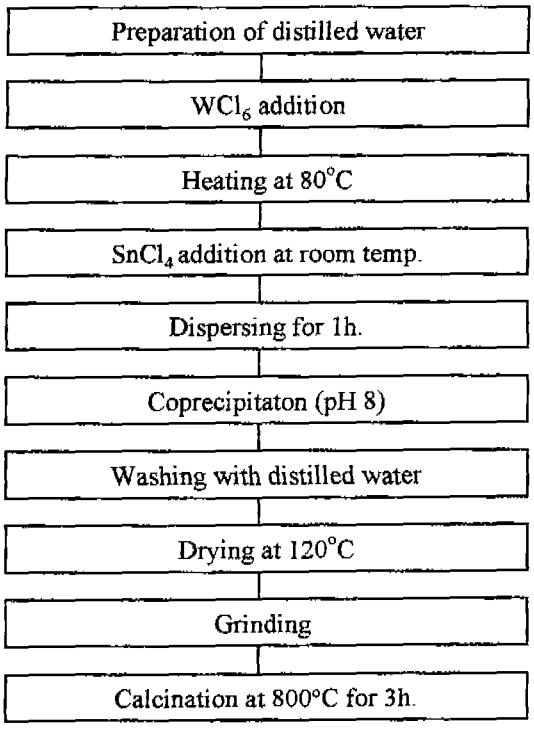

Fig. 1. Flow chart of manufacture process of W doped SnO_2 powder.

ture process of W doped SnO_2 powders. WCl_6 was dissolved in the distilled water heated at 80°C, and then, $SnCl_4$ was added in the aqueous solution. The $SnCl_4$ and WCl_6 aqueous solution was neutralized with NH_4OH to obtain coprecipitate of W doped tin oxide hydrate. After the copreapitate was thoroughly washed with distilled water to remove residual ammonium and chlorine ions, it was dried and calcined in air. Fig. 2 shows XRD patterns of the precipitate with calcination temperature from 500°C to 800°C. The as-received precipitate was amorphous. Diffraction peaks corresponding to polycrystalline SnO_2, however, appeared after calcination of the precipitate at the temperatures above 500°C. The precipitate was well crystallized with increase of calcination temperatures, and diffraction peaks of the precipitate calcined at 800°C for 3 h were exactly fit to those of commercial SnO_2 powder.

On the other hand, the ceramic mixture WO_3(5 wt%)/SnO_2, which was suggested by Yun *et al.*,[8] was prepared using commercial WO_3 and SnO_2 powders(99.99%, Aldrich Co.) for comparative study with our coprecipitated powder. The average grain sizes of our coprecipitated powder and

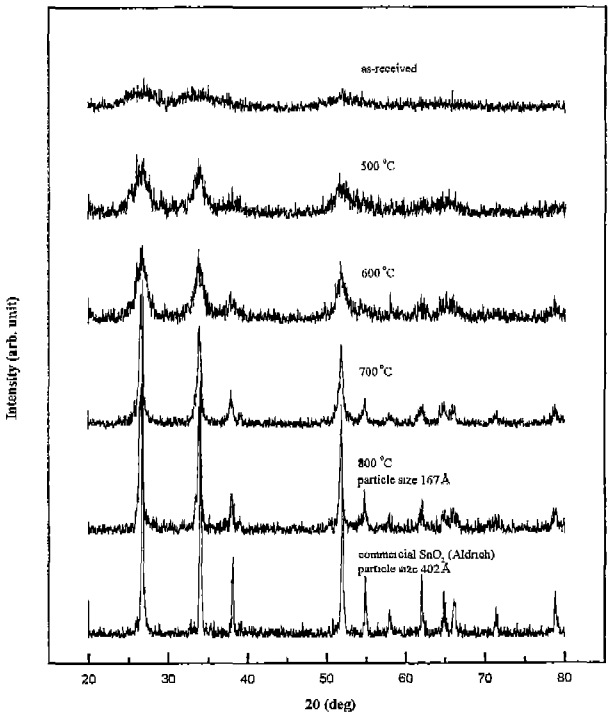

Fig. 2. XRD patterns of precipitate with calcination temperatures from 500°C to 800°C.

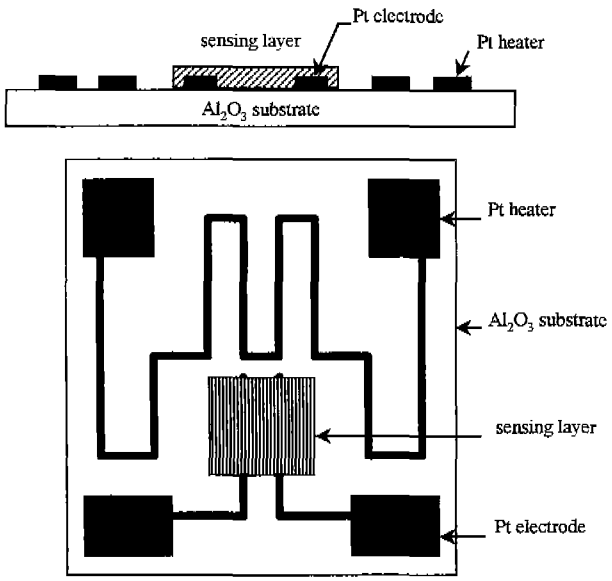

Fig. 3. Schematic diagram of thick film gas sensor.

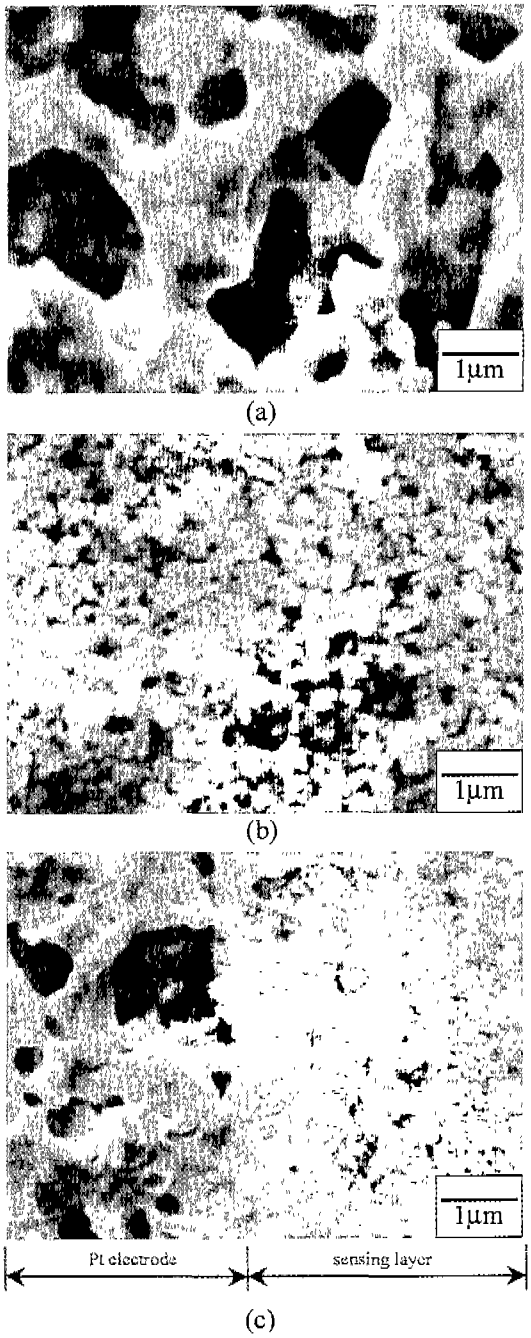

Fig. 4. SEM micrographs of (a) Pt electrode, (b) sensing layer, and (c) interface of electrode/sensing layer.

commercial SnO_2 powder were around 20 nm and 40 nm, respectively, through calculation from XRD data using the Scherrer equation.

2.2. Fabrication of sensor

Fig. 3 shows the schematic view of our thick film gas sensor consisting of a sensing layer, electrodes, and heater formed on Al_2O_3 substrate by a screen printing technique. The sensor fabrication procedure was as follows.

i) formation of Pt patterns on alumina substrate of 3.5×3.5 mm^2 for electrodes and heater. (fired at 1100°C for 1h in air)

ii) paste preparation by thoroughly mixing the sensing materials(powders) with an organic binder.

iii) printing of sensing layer in thickness of about 5 μm.

The printed sensing layer was heated at 150°C for 30 minutes to eliminate organic binder, sintered at 600°C for 1h to improve the adhesion between the SnO_2 particles and Al_2O_3 substrate, and then fired at 800°C for 30 minutes along with Pt wire bonding. The fabricated sensing layer was 1.0×1.0 mm^2 in size and distance of two electrodes was 0.2 mm. Fig. 4 shows scanning electron microscope micrographs of the fabricated Pt electrode, sensing layer, and interface of electrode/sensing layer. The sintered Pt electrode had very rough structure with large pores. In addition, the sensing layer consisted of relatively fine particles was spread into the skeleton of Pt electrode. This kind of binding between metal electrode and ceramic layer improved the mechanical strength of the interface due to three dimensional interlocking and produced large interfacial areas. Since lots of interfacial contacts between Pt electrode and sensing layer were formed, it was expected that contact resistance electrode/sensing layer was largely diminished compared with one of sensing layer itself. On the other hand, the sensing layer had lots of fine pores. This desirable porous structure enlarges the surface area of sensing layer, which means increase of adsorption site. Since the sensing mechanism of gas sensor is based on gas adsorption on the ceramic surface, the increase of adsorption site is important to improve the sensitivity to pollutant gases. The thick film gas sensor as shown in Fig. 3 was packed with plastic capsule after Pt wire bonding.

Table 1 shows variation of resistance of W doped SnO_2 sensing layer with W concentration. The resistance of the fabricated sensing layer as described above was measured

Table 1. Resistance of SnO_2 Sensing Layer with W Concentration

W concentration	Resistance of sensing film (at room temperature)
5 mol% (7.5 wt%) doped SnO_2	1~10 K Ω
1 mol% (1.5 wt%) doped SnO_2	100~1000 K Ω
0.5 mol% (0.8 wt%) doped SnO_2	10~20 M Ω
0.1 mol% (0.15 wt%) doped SnO_2	>>30 M Ω
WO_3(5 wt%) mixed SnO_2	>>30 M Ω

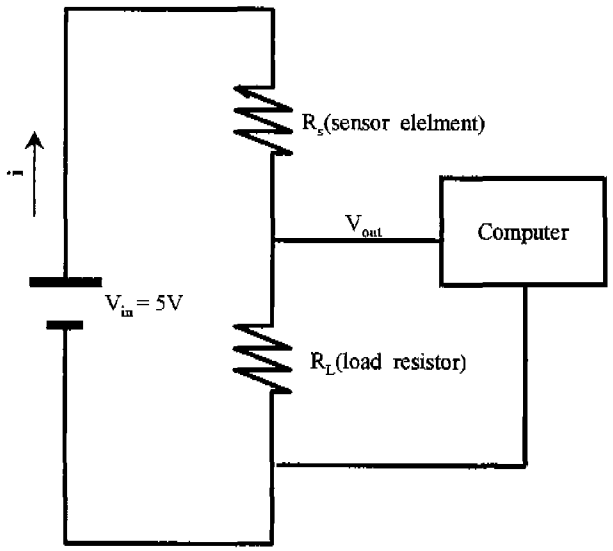

Fig. 5. Schematic diagram of measurement circuit.

by digital tester. The resistance of SnO_2 sensing layer with small W doping below 0.1 mol% showed very high resistance at room temperature, on the other hand, that of W doped SnO_2 sensing layer with W content over 0.1 mol% showed relatively low resistance. The decrease of resistance with increase of W doping concentration was attributed to increase of carrier electron, because W(+6) behaved as a donor in SnO_2 crystal. Since base resistance of sensing layer drastically decreases at operation temperature of 300°C, it is hard to measure the change of the electrical resistance of the sensing layer on the exposure to pollutant gases. In this reason, W(0.1 mol%) doped SnO_2 sensing layer was selected as a sample for the comparative study with WO_3(5 wt%) mixed SnO_2 suggested by Yun.[8]

2.3 Measurement of long-term stability and sensitivity

To compare long-term stability between WO_3 mixed and W doped SnO_2 gas sensor, the input circuit voltage 5 V was applied across RS(sensor element) and RL(load resistor), and the change of Vout voltage was continuously recorded with operating time. Fig. 5 shows a schematic of the measurement circuit. The operation temperature of the sensing layer was maintained at 300°C, because this temperature showed high sensitivities to various gases. In order to compare relative sensitivities of two types of sensors alcohol, acetone, and cigarette smoke were used as test gases. The gas sensitivity(ΔV) was defined as $V_{out,gas}$-$V_{out,air}$, where $V_{out,gas}$ and $V_{out,air}$ are the voltage of V_{out} in test gas and air, respectively.

III. Results and Discussion

3.1. Long-term stability

Fig. 6 shows the variations of the Vout voltage of two types of sensors with operating time at 300°C in air. The ini-

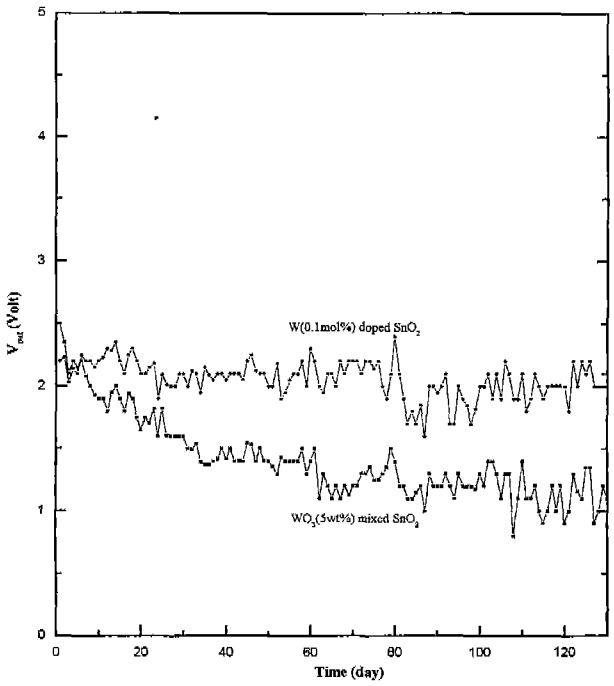

Fig. 6. Variation of the V_{out} voltage of two types of sensors with operating time.

tial Vout voltage of W doped SnO_2 and WO_3 mixed SnO_2 gas sensor were 2.5 V and 2.2 V, respectively. Whereas the Vout of WO_3 mixed SnO_2 gas sensor was gradually decreased with operating time, that of W doped SnO_2 gas sensor was maintained along with operating time. The fluctuations of Vout voltage in Fig. 6 was attributed to the variation of temperature and humidity of ambient air. This result suggests that two types of sensors had different electric conduction mechanisms. The electrical conduction of WO_3 mixed SnO_2 was dominated by nonstoichiometry, because SnO_2 was a major and continuous phase and had the nonstoichiometric composition generally associated with oxygen vacancies. The carrier electrons were produced due to the oxygen vacancies as follows.

$$Sn^{+4}{}_{2\beta}e^{-}{}_{\beta}O^{-2}{}_{2-\beta}\ (V_o = V_o + 2e^{-}) \quad (1)$$

The oxygen vacancies of SnO_2, however, reacted with an ambient oxygen gas at operation temperature, and the vacancy concentration varied toward an equilibrium status compatible with the ambient oxygen pressure and temperature. Since equilibrium oxygen partial pressure with SnO_2 is extremely low from a thermodynamic point of view, ambient oxygen partial pressure of about 0.2 atm caused the forward reaction of following equation, and thus, diminished the oxygen vacancies in SnO_2.

$$V_o + 1/2O_2(g) = O_o \quad (2)$$

In this reason, it was hard to constantly keep the base resistance of WO_3 mixed SnO_2. In addition, the resistance of SnO_2 steadily increased with operating time. On the other hand, the conduction mechanism of W doped SnO_2 gas sensor was dominated by controlled valence mechanism in stead of nonstoichiometry as follows.

$$Sn^{+4}{}_{1-x}2e^{-}{}_{x}W^{+6}{}_{x}O^{-2}{}_{2} \quad (3)$$

This means that the resistance of W doped SnO_2 gas sensor was controlled mainly by the dose of tungsten without large regarding of oxygen vacancy concentration. Even though the oxygen vacancies remained in SnO_2 reacted with ambient oxygen gas, the effect was not so enough as to change the whole resistance of W doped SnO_2 sensor. Consequently, the long-term stability could be obtained.

3.2 Sensitivity

Fig. 7 shows relative sensitivities of two types of sensors to pollutant gases such as acetone, alcohol, and cigarette smoke. In this figure, W(0.1 mol%) doped SnO_2 gas sensor had higher sensitivities to both acetone and alcohol compared with WO_3(5 wt%) mixed SnO_2 gas sensor. This result was considered to be due to the smaller grain size of our coprecipitated powder(~20 nm) than one of the commercial SnO_2 powder for the WO_3 mixed SnO_2 gas sensor(~40 nm). On the other hand, WO_3(5 wt%) mixed SnO_2 gas sensor showed higher sensitivity to cigarette smoke. WO_3 material has especially high sensitivity to H_2S gas, which is one of principal elements of cigarette smoke. The following equation shows the reaction of WO_3 with H_2S gas.[9]

$$3WO_3(s) + 7H_2S(g) \rightarrow 3WS_2(s) + SO_2(g) + 7H_2O(g) \quad (4)$$

For our sensors the oxygen vacancies were created by the reaction of WO_3 with H_2S, and thus, the resistances of the gas sensors largely decreased. In this reason, WO_3(5 wt%) mixed SnO_2 gas sensor showed higher sensitivity due to the comparatively larger W content compared with W(0.1 mol%) doped SnO_2 gas sensor.

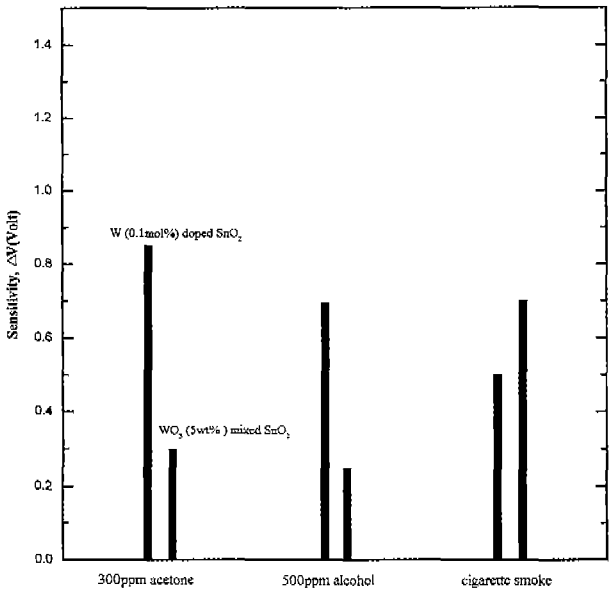

Fig. 7. Comparative sensitivities(ΔV) of two types of sensors to several gases ($\Delta V = V_{out\ gas} - V_{out\ air}$).

IV. Conclusions

Through this study, we believe the small amount of W(~0.1 mol%) doping into SnO_2 improved long-term stability, which has been a principal problem generally taking place in SnO_2 semiconductor gas sensor. The W doped SnO_2 sensing material could be successfully prepared by coprecipitation method. W(0.1 mol%) doped SnO_2 gas sensor fabricated in this work showed higher gas sensitivities to both acetone and alcohol compared with WO_3(5 wt%) mixed SnO_2 gas sensor. The WO_3(5 wt%) mixed SnO_2 gas sensor, however, showed more superior sensitivity to cigarette smoke due to the larger W content. It is expected that the gas sensor possessing the excellent performance to pollutant gases can be obtained by the adjustment of total WO_3 content with small amount of W doping into SnO_2.

References

1. M. Egashira and Y. Shimizu, "Odor Sensing by Semiconductor Metal Oxides," Sensors and Actuators B, **13-14**, 443-446 (1993).
2. T. Maekawa, J. Tamaki, N. Miura and N. Yamazoe, "Development of SnO_2-based Ethanol Gas Sensor," Sensors and Actuaors B, **6**, 63-69 (1992).
3. L. Daza, S. Dassy and B. Delmon, "Chemical Sensor Based on SnO_2 and WO_3 for the Detection of Formaldehyde: Cooperative Effects," Sensors and Actuators B, **10**, 99-105 (1993).
4. K. Suzuki and T. Takada, "Highly Sensitivity Odour Sensors Using Various SnO_2 Thick Films," Sensors and Actuators B, **24-25**, 773-776 (1995).
5. G. S. Devi, S. Manorama and V. J. Rao, "High Sensitivity and Selectivity of an SnO_2 Sensor to H_2S at Aroud 100°C," Sensors and Actuators B, **28**, 31-37 (1995).
6. H. M. Lin, C. M. Hsu, H. Y. Yang, P. Y. Lee and C. C. Yang, Nanocrystalline WO_3-based H_2S Sensors, Sensors and Actuators B, **22**, 63-68 (1994).
7. E. P. S. Barrett, G. C. Georgiades and P. A. Sermon, "The Mechanism of Operation of WO_3-based H_2S Sensors," Sensors and Actuators B, **1**, 116-120 (1990).
8. D. H. Yun, C. H. Kwon, H. K. Hong, H. W. Shin, S. R. Kim, and K. Lee, "Abnormal Current-voltage Characteristics of WO_3-doped SnO_2 Oxide Semiconductors and Their Applications to Gas Sensors," Senors and Actuators B, **35-36**, 48-51 (1996).
9. B. Fruhberger, M. Grunze and D. J. Dwyer, "Surface Chemistry of H_2S-sensitivity Tungsten Oxide Films," Sensors and Actuators B, **31**, 167-174 (1996).